Journal of Power Sources 226 (2013) 329–333

Contents lists available at SciVerse ScienceDirect

Journal of Power Sources

journal homepage: www.elsevier.com/locate/jpowsour

Short communication

Poly(ethylenglycol)dimethylether–lithium bis(trifluoromethanesulfonyl)imide, PEG500DME–LiTFSI, as high viscosity electrolyte for lithium ion batteries

Rebecca Bernhard [b], Alessandro Latini [a], Stefania Panero [a], Bruno Scrosati [a], Jusef Hassoun [a,*]

[a] Department of Chemistry, Sapienza University, Piazzale Aldo Moro 5, 00185 Rome, Italy
[b] Department of Chemistry, TU München, Lehrstuhl für Technische Elektrochemie

HIGHLIGHTS

- A PEG500DME–LiTFSI high viscosity, safe electrolyte is here reported.
- The electrolyte shows enhanced electrochemical properties.
- A battery using TiO_2 anode, $LiCoO_2$ cathode and the electrolyte is studied.
- The 2 V-battery is characterized by high stability and low polarization.
- The electrolyte is a promising candidate for application in Li-ion battery.

ARTICLE INFO

Article history:
Received 4 October 2012
Received in revised form
14 October 2012
Accepted 15 October 2012
Available online 10 November 2012

Keywords:
Poly(ethyleneglycol)dimethylether
Lithium bis(trifluoromethanesulfonyl)imide
PEG500DME–LiTFSI
Safe-electrolyte
Lithium ion battery

ABSTRACT

In this paper we report a poly(ethylenglycol)dimethylether–lithium bis(trifluoromethanesulfonyl) imide (PEG500DME–LiTFSI) as high viscosity, safe electrolyte for lithium ion batteries. The high molecular weight of the end-capped ether solvent is reflected as low vapor pressure and excellent thermal stability of the electrolyte, as demonstrated by thermogravimetry, this resulting in remarkable safety content. The electrochemical impedance spectroscopy study of the electrolyte demonstrates a Li-transference number of 0.48, a conductivity of the order of 10^{-3} S cm^{-1}, and a high interphase stability with the lithium metal, the linear sweep voltammetry indicates an electrochemical stability window extending up to 4.8 V vs. Li/Li$^+$. Furthermore, promising electrochemical performances in terms of reversibility, cycling stability and low charge–discharge polarization are observed using the electrolyte in lithium and in lithium ion batteries using lithium cobalt oxide (LCO) as cathode and titanium dioxide (TiO_2) as anode. Hence, this electrolyte is a promising candidate for applications in safe, high performance lithium ion batteries.

1. Introduction

Storage applications for electrical energy bear an important role in this century. In this respect lithium ion batteries, now largely used in the portable devices, are considered the most promising candidates as power supplies for hybrid electric vehicles (HEVs), plugged-in hybrid vehicles (PHEVs), full electric vehicles (EVs), as well side systems for renewable energies production plants, such as those based on wind and solar power. However, improvements in terms of safety and cost [1–3] are still needed in order to match the severe targets required by these emerging markets. Safety concerns are mainly associated with the high flammability of the volatile carbonated organic electrolytes commonly used in lithium ion batteries with consequent risks of thermal runaway leading to fire or even explosive hazards [4]. Valid alternative electrolytes, characterized by low cost and high safety content, are those based on poly(ethyleneoxide), (PEO) [3]. PEO-based electrolytes in their solid amorphous state demonstrated favorable properties, such as good ionic conductivity [5], satisfactory electrochemical and interfacial stability [6] and excellent mechanical properties [5,7]. Liquid, highly viscous glymes were studied in the late 1990s by Shi et al. (1995) and Appetecchi et al. (1996) [8,9]. The results demonstrate that these electrolytes can be safely used in lithium cells. However, to fully assume cell safety, the use of anodes operating at voltages values that avoid the electrolyte decomposition is recommended. Relevant examples are lithium titanium oxide ($LiTi_5O_{12}$, LTO) and titanium dioxide (TiO_2) [10,11], that are characterized by a working voltage ranging between 1.0 and 1.5 V vs. Li/Li$^+$ [12,13].

In this scenario it has appeared to us of interest to investigate the thermal and the electrochemical properties of an electrolyte

* Corresponding author. Tel.: +39 (0)6 49913530; fax: +39 (0)6 491769.
E-mail address: jusef.hassoun@uniroma1.it (J. Hassoun).

0378-7753/$ – see front matter © 2012 Elsevier B.V. All rights reserved.
http://dx.doi.org/10.1016/j.jpowsour.2012.10.059

formed by dissolving a lithium-bis-(trifluormethanesulfonyl)-imide, LiTFSI, salt in a high viscosity poly(ethylenglycol)dimethylether (with 500 g molecular weight), PEG500DME, solvent. Thermo-gravimetric analysis (TGA) and differential scanning calorimetry (DSC) are used as preferred techniques for the characterization of the thermal properties of the electrolyte and linear sweep voltammetry (LSV) and electrochemical impedance spectroscopy (EIS) for the characterization of the electrochemical behavior. The PEG500DME–LiTFSI electrolyte is then tested in a full cell coupling a TiO_2 anode and a $LiCoO_2$ cathode to form a new, advanced configuration lithium ion battery.

2. Experimental

Before mixing, the solvent PEG500DME was dried for several hours under vacuum until the water content was below 15 ppm. The electrolyte solution was prepared by mixing Poly(ethyleneglycol) 500–Dimethylether (PEG500DME; $M = 500$ g mol^{-1}) (Sigma Aldrich) and lithium-bis-(trifluormethanesulfonyl)-imide (Sigma Aldrich) (LiTFSI) in a 1 mol kg^{-1} ratio in an argon filled glovebox (<1 ppm water). The electrolyte is here identified with the acronym PEG500DME–LiTFSI.

The anodic and cathodic stability window of the electrolyte was studied by linear sweep voltammetry using a Biologic VMP3 instrument at a scan rate of 0.2 mV s^{-1} in a three-electrode cell, using lithium metal as a counter and reference electrode and Super P carbon (Timcal) working electrode on aluminum and copper current collector, respectively, in the 0.01–5.0 V potential range.

Lithium–lithium symmetrical Swagelok and blocking electrodes cell (Metrohm) were used for lithium interface stability and conductivity measurements, respectively. The results were carried out by electrochemical impedance spectroscopy (EIS). The related error bars were calculated by distribution analysis taking into account the error associated with the temperature, the resistance, and the cell constant. The determination of the lithium transference number was obtained using a symmetrical lithium–lithium cell, by a combination of AC and DC polarization pulses according to Bruce & Vincent method [14]. The determination of the initial and steady state resistance was done by a nonlinear least squares fit analysis (NLLSQ) reported by Boukamp [15,16]. The impedance spectra were performed by using VersaSTATMC (Princeton applied research) in frequency range of 500 kHz to 10 mHz using a 10 mV AC-signal amplitude and a 30 mV DC pulse (for transference number measurement).

The thermal characteristics of the electrolyte solution were determined by thermo-gravimetric analysis (TGA) in nitrogen stream within a temperature range of 25 °C and 500 °C with a heating rate of 10 °C min^{-1} (Mettler Toledo TGA/SDTA 851) and by differential scanning calorimetry (DSC) in sealed aluminum pans under nitrogen atmosphere at a cooling/heating rate of 10 °C min^{-1} (Mettler Toledo DSC821^e). The chosen protocol for the DSC measurement was constituted by a first cooling scan from 25 °C to −95 °C followed by heating up to 90 °C and again a cooling back to 25 °C.

The lithium stripping/deposition test was performed in a symmetrical Li/PEG500DME–LiTFSI/Li cell galvanostatically controlled at 0.1 mA over 500 cycles by using a MACCOR Series 4000 Battery test system (Maccor Inc.).

Swagelok, T-type lithium half cells using titanium dioxide (TiO_2) and lithium cobalt oxide ($LiCoO_2$; LCO) electrodes, as well as the full cell combining the two electrodes in the PEG500DME–LiTFSI electrolyte soaked in a Whatman® glass fiber separator, were characterized at C/5 (34 mA g^{-1}) under galvanostatic cycling using MACCOR Series 4000 Battery Test System (Maccor Inc.). The TiO_2 and $LiCoO_2$ electrodes were coated on copper and on aluminum current collectors, respectively. The anatase type TiO_2 was synthesized as reported by Chen et al. [17], while the LCO was a commercial available powder supplied by Nippon Chem. Industrial Co. Ltd Tokyo, Japan. Both the electrodes were composed of active material powder, Super P carbon and PVDF binder (Solvay) in an 80:10:10 weight ratio. Slurries of these mixtures in N-methyl-2-pyrrolidone (Aldrich) were cast on the above mentioned current collectors. The density of dried electrodes was 4 mg cm^{-2} and 6 mg cm^{-2} for TiO_2 and for LCO, respectively.

3. Result and discussion

Fig. 1A shows the electrochemical stability window of the PEGDME500-LiTFSI electrolyte in the range 0.01–5.0 V Li/Li$^+$ (A) and its lithium interface stability over time (B). The anodic stability is warranted until 4.8 V vs. Li/Li$^+$ beyond which electrolyte decomposition does occur. The cathodic scan shows stability down to 1.5 V vs. Li/Li$^+$. At the lower voltages, i.e. in the range of 1.2–0.7 V vs. Li/Li$^+$, peaks associated with the solid electrolyte interface (SEI)

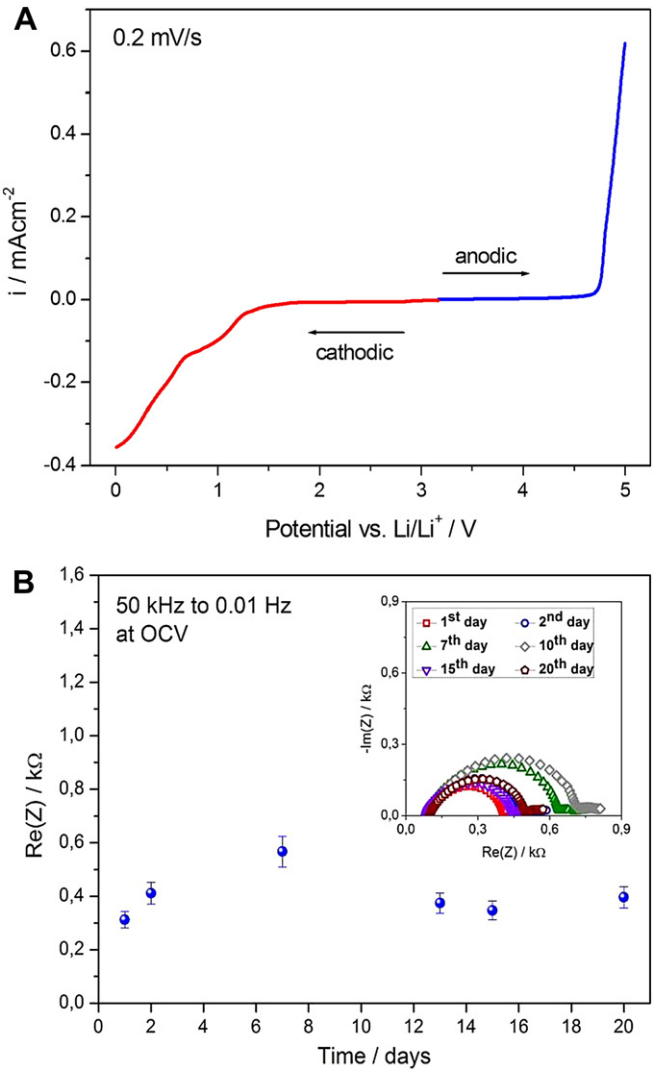

Fig. 1. A: Current vs. potential profile of the linear sweep voltammetry (LSV) performed using the Li/PEG500DME–LiTFSI/SP cell in the 0.01–5.0 V vs. Li/Li$^+$ window at 0.2 mV s^{-1} and room temperature for the determination of the electrochemical stability window of the electrolyte. B: Time dependence of the overall resistance measured by electrochemical impedance spectroscopy (EIS) of the symmetrical Li/PEG500DME–LiTFSI/Li cell, with in inset some of the corresponding Nyquist plots. 500 kHz to 10 mHz frequency range, 10 mV signal amplitude, room T.

film formation [18] and with the occurrence of intercalation of lithium ions in the amorphous carbon structure, at voltage value lower than 0.5 V, are observed. Fig. 1B shows the variation of the overall resistance of the symmetrical Li/PEO500DME–LiTFSI/Li cell over several days. The corresponding impedance spectra in the inset of the figure demonstrate that during the first days the resistance increases up to a maximum of 640 Ω to then decrease to 310 Ω, matching the pristine value. In the final part of the test, the resistance increases again as expected due to the SEI film formation-re-dissolution process [18].

As well known, the ionic conductivity depends on temperature due to the change of the ions mobility. Fig. 2, reporting the Arrhenius plot in the 100 °C–25 °C temperature range of the PEG500DME–LiTFSI (1 m) electrolyte, evidences that the ionic conductivity ranges from 4×10^{-3} S cm^{-1} at ca. 100 °C to 0.45×10^{-3} S cm^{-1} at RT, i.e. at values well matching those required for the application in lithium battery. Furthermore, the figure shows a good overlapping between the heating and the cooling scans, this indicating a good thermal stability.

Fig. 3A illustrates the TGA profile of the electrolyte. A first massive weight loss at around 250 °C associated with the PEG500DME solvent evaporation and following weight loss at around 350 °C associated with the LiTFSI decomposition and removal [19] are observed. Therefore, on the basis of these data we can conclude that the electrolyte mixture here reported has a thermal stability extending up 200 °C. The low temperature thermal behavior of the PEG500DME–LiTFSI electrolyte, evidenced by the DSC traces reported in Fig. 3B, shows a phase change from liquid to solid at around 4 °C and a glass transition at −70/−80 °C.

The lithium transference number (t_{Li+}) is fundamental for battery characterization. This is a dimensionless parameter describing the fraction of the overall charge which is transported by lithium ions, assuming a value ranging from 0 to 1 depending on the diffusion of the ions through the electrolyte during the electrochemical process. Fig. 4 shows the DC current versus time profile and, in the inset, the impedance spectra at the initial and the steady state of the Li/PEG500DME–LiTFSI/Li symmetrical cell. Using these data the lithium transference number of the PEG500DME-based

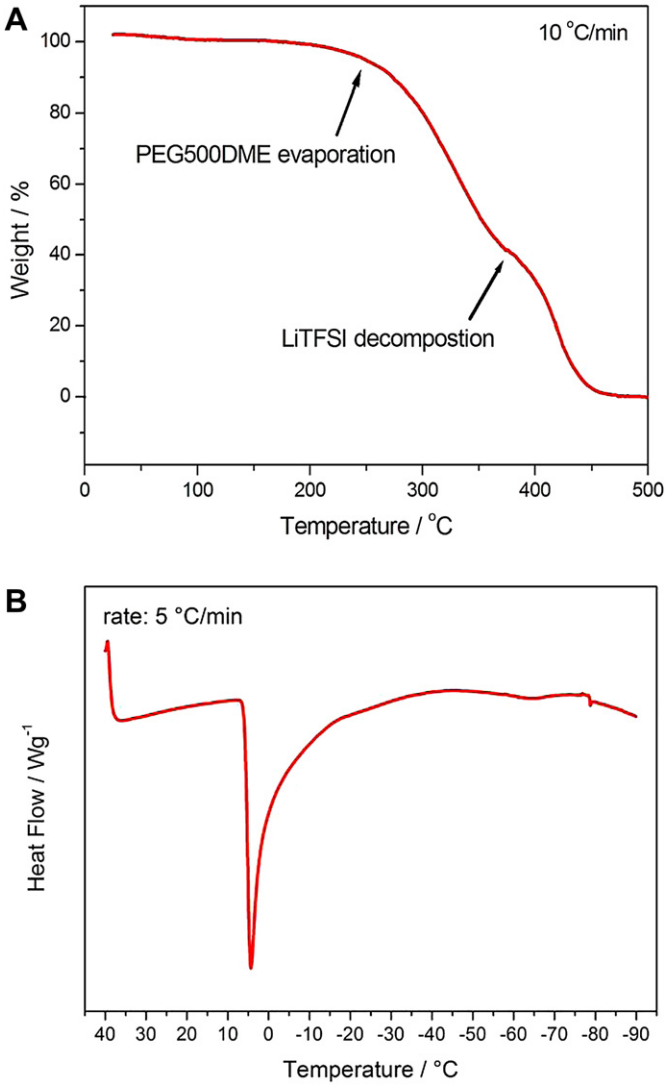

Fig. 3. A: Thermo-gravimetric analysis (TGA) profile of the PEG500DME–LiTFSI from 25 °C to 500 °C under nitrogen flow. B: Differential scanning calorimetry (DSC) traces of the electrolyte at a 5 °C min^{-1} rate.

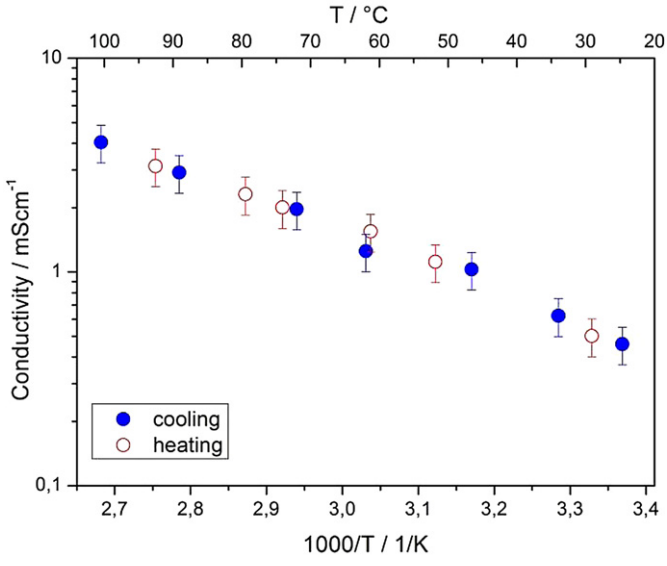

Fig. 2. Temperature dependence of the ionic conductivity, i.e. Arrhenius plot, of the PEG500DME–LiTFSI electrolyte reported in this paper. The single point conductivity has been obtained by measuring the resistance using a conductivity cell with predetermined cell constant, by employing the electrochemical impedance spectroscopy in the 500 kHz to 10 mHz frequency window with a 10 mV signal amplitude.

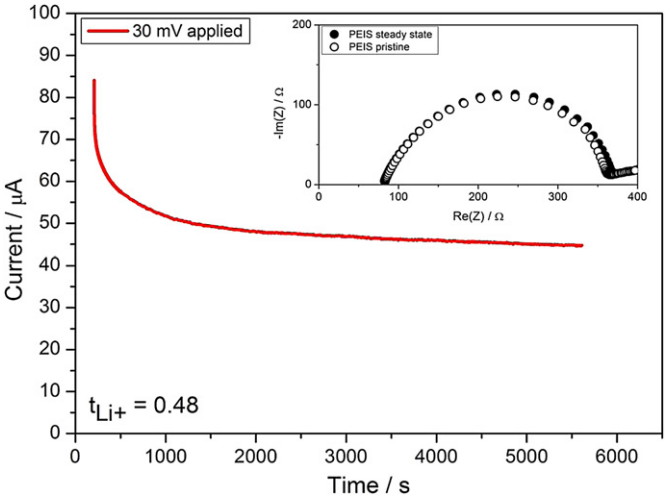

Fig. 4. AC/DC characterization used for the lithium transference number determination. Voltage vs. time profile upon application of 30 mV DC signal to a symmetric Li/PEG500DME–LiTFSI/Li cell until stabilization with, in inset, the Nyquist profiles corresponding to the EIS measurement performed at the initial and the steady state condition.

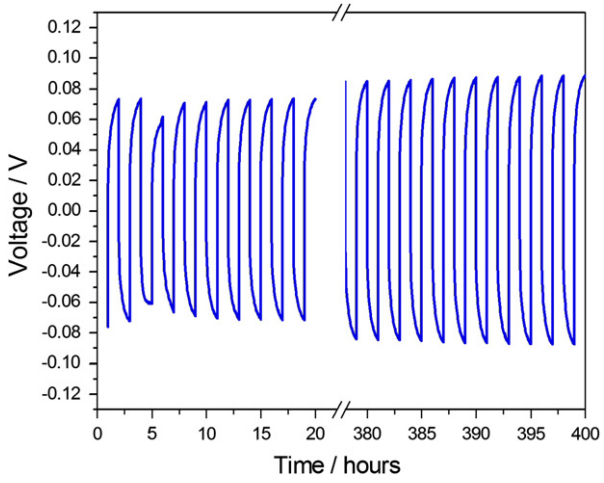

Fig. 5. Stable and symmetrical voltage vs. time profile of lithium deposition/stripping galvanostatic test performed applying a 0.1 mA current to the Li/PEG500DME–LiTFSI/Li cell over 200 cycles.

electrolyte here developed is calculated according to Bruce–Vincent equation equal to $t_{Li+} = 0.48$ by, i.e. a value very well comparing, if not superior, than that of others PEG500DME-based electrolytes [20]. We believe that this high t_{Li+} value is due to the combined effect of the enhanced solvating properties of the PEG500DME liquid and the excellent mobility of the Li^+ ions originated from the LiTFSI salt.

Fig. 5 reports the evolution of a lithium deposition/stripping test carried out in a symmetrical Li/PEG500DME–LiTFSI/Li cell by monitoring the overvoltage over time. The voltage vs. time profile shows a limited polarization, i.e. of about 85 mV over 200 cycles. These values are convincing in demonstrating the compatibility of the electrolyte with the lithium electrode.

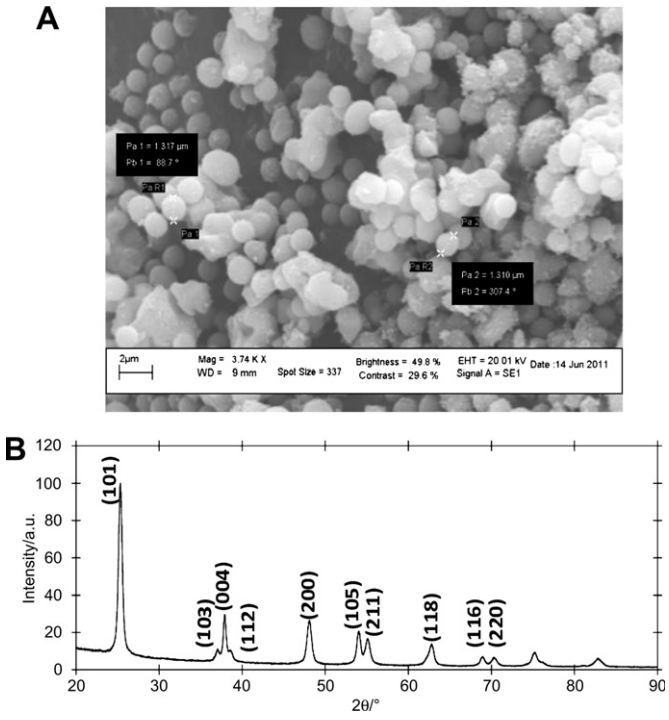

Fig. 6. A: Scanning electron microscopy (SEM) image of the TiO_2 here synthesized showing the spherical particles morphology with an average size of 1 μm. B: XRD pattern with typical signatures attributed to the anatase TiO_2 phase.

The behavior of the PEG500DME–LiTFSI electrolyte in a lithium ion cell was determinate by combining it with a commercial $LiCoO_2$ cathode and a TiO_2 anode synthesized in our laboratory. Prior to its use, the TiO_2 powder was characterized by scanning electron

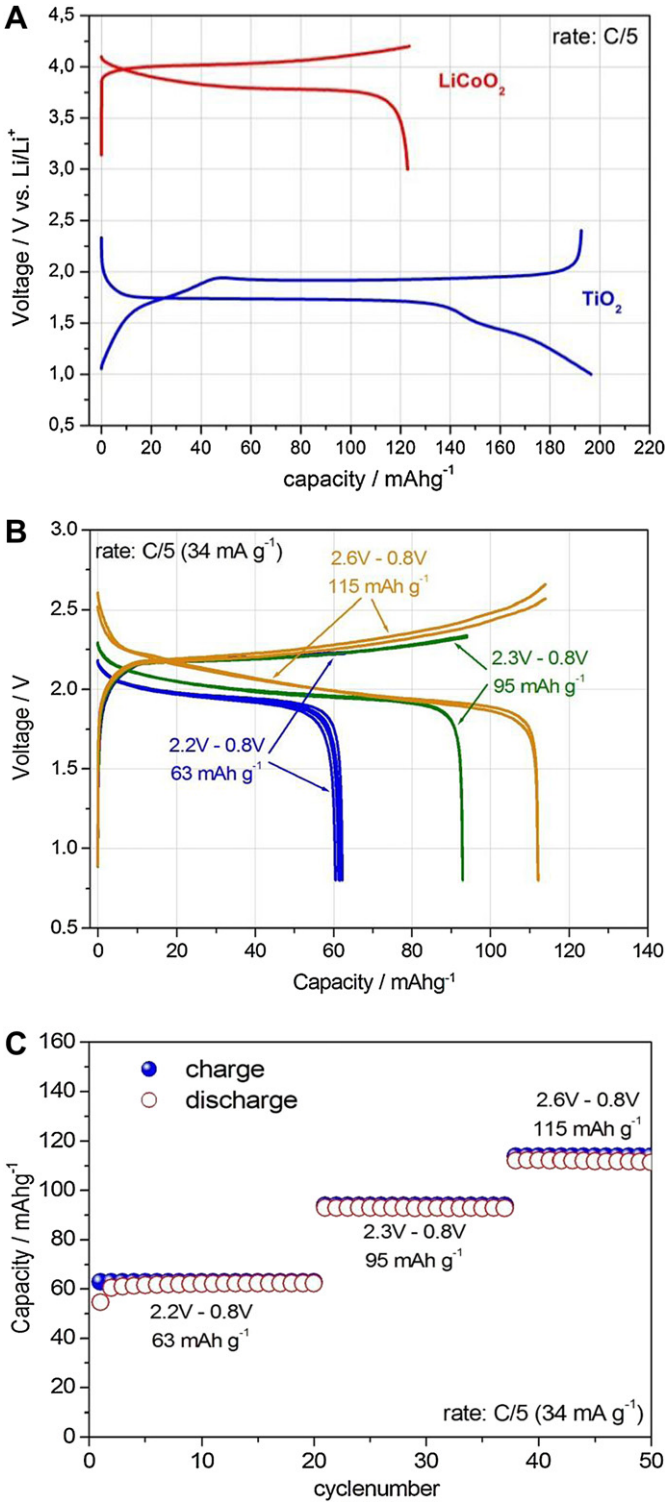

Fig. 7. A: Typical voltage profiles, in comparison, for the half lithium cells prepared using the TiO_2 and the $LiCoO_2$ electrodes in the PEG500DME–LiTFSI electrolyte and cycled at a C/5 (34 mA g^{-1}) rate at the fifth charge/discharge cycle. B: Voltage profiles of the cycling tests performed on the TiO_2/PEG500DME–LiTFSI/$LiCoO_2$ full cell at three different capacity/voltage limits with a current of 34 mA g^{-1}. C: Cycling behavior over 50 cycles of the TiO_2/PEG500DME–LiTFSI/$LiCoO_2$ full cell.

microscopy (SEM) and X-ray diffraction (XRD). Fig. 6A evidences the particular morphology of this powder based on spherical particles with a monodisperse size of around 1 μm. The Rietveld-analysis of the XRD reported in Fig. 6B reveals specific peaks assigned to a pure anatase phase [21], with cell parameters calculated as $a = b = 3.7849$ Å, $c = 9.4955$ Å with a crystallite size of ca. 20 nm. Finally, Brunauer–Emmett–Teller (BET) analysis of the TiO_2 powder (data not reported) gave a specific surface area of 73.0 ± 0.2 m^2 g^{-1}, this confirming the nanoporous morphology of the material. To be noticed that the specific area obtained by considering only the external geometric surface of the 1 μm-spheres, see SEM in Fig. 6A, is calculated to be of the order of 1.5 m^2 g^{-1}, i.e. a much less value than that observed by BET analysis.

Fig. 7A reports the typical voltage profile of the TiO_2 and the LCO half cells in the PEG500DME–LiTFSI electrolyte performed at a C/5 rate evidencing a specific capacity of 195 mAh g^{-1} and of 120 mAh g^{-1} for the TiO_2 and for the LCO, respectively, with coulombic efficiency exceeding 98% for both the electrodes, and voltage signatures reflecting the following processes:

$$TiO_2 + xLi^+ + xe^- = Li_xTiO_2 \ (x = 0.6) \quad (1)$$

$$LiCoO_2 = Li_{(1-x)}CoO_2 + xLi^+ + xe^- \ (x = 0.45) \quad (2)$$

As observed in Fig. 7A, and considering the reaction mechanisms (1) and (2), we see that the anode capacity exceeds that of the cathode. This difference is taken under consideration for assuring proper cell balance. Fig. 7B, reporting the cycling behavior of the full TiO_2/PEG500DME–LiTFSI/LCO cell performed at various voltage cutoff and at a rate of C/5 (34 mA g^{-1} current), clearly demonstrates that the cell operates well with a voltage value centered at about 2.0 V, as expected by the combination of the voltage signature of the two electrodes reported in Fig. 7A, showing good capacity and coulombic efficiency values. The above described test was carried out by monitoring the charge capacity to determine the best voltage cutoff to be applied for assuring an efficient application in this lithium ion cell. This value is found to be of 2.6 V. Fig. 7C, reporting the capacity versus cycles profile corresponding to the above described cell, evidences a good cycle life, extending over 50 cycles, and an excellent charge/discharge coulombic efficiency.

4. Conclusion

The poly(ethylenglycol)dimethylether–lithium bis(trifluorome thanesulfonyl)imide electrolyte reported in this paper evidenced a high thermal and electrochemical stability. These favorable properties allowed the application of the PEG500DME–LiTFSI electrolyte in a lithium ion battery in combination with a titanium dioxide (TiO_2) anode and a lithium cobalt oxide ($LiCoO_2$) cathode. The TiO_2/PEG500DME–LiTFSI/$LiCoO_2$ battery evidenced good behavior, both in terms of capacity and of cycling stability, this suggesting the applicability of the electrolyte in safe, advanced configuration lithium ion batteries.

Acknowledgments

This work was carried out within the SEED Project “REALIST” sponsored by Italian Institute of Technology (IIT). The authors thank Professor Hubert A. Gasteiger from the Department of Chemistry, TU München, Lehrstuhl für Technische Elektrochemie for the kind collaboration.

References

[1] H. Horie, T. Abe, T. Kinoshita, Y. Shimoida, World Electric Vehicle J. 2 (2008) 25–31.
[2] J.-M. Tarascon, M. Armand, Nature 414 (2001) 359.
[3] P.G. Bruce, B. Scrosati, J.-M. Tarascon, Angew. Chem. 120 (2008) 2972.
[4] M. Wakihara, O. Yamamato (Eds.), Lithium Ion Batteries, Kodansha-Wiley, Tokyo, 1998.
[5] G.B. Appetecchi, J. Hassoun, B. Scrosati, F. Croce, F. Cassel, M. Salamon, J. Power Sources 124 (2003) 246.
[6] H.-M. Xiong, K.-K. Zhao, X. Zhao, Y.-W. Wang, J.S. Chen, Solid State Ion. 159 (2003) 89.
[7] W. Wieczorek, D. Raducha, A. Zalewska, J.R. Stevens, J. Phys. Chem. 102 (1998) 8725.
[8] J. Shi, M. Malservisi, B. Marsan, Electrochim. Acta 40 (1995) 2425.
[9] G.B. Appetecchi, G. Dautzenberg, B. Scrosati, J. Electrochem. Soc. 143 (1996) 6.
[10] F.-F. Cao, X.-L. Wu, S. Xin, Y.G. Guo, L.-J. Wan, J. Phys. Chem. C 114 (2010) 10308.
[11] S. Brutti, V. Gentili, P. Reale, L. Carbone, S. Panero, J. Power Sources 196 (2011) 9792.
[12] K. Ozawa, Li-ion Rechargeable Batteries, Wiley VCH Weinheim, Germany, 2009.
[13] K. Zaghib, M. Dontigny, A. Guerfi, P. Charest, I. Rodrigues, A. Mauger, J. Power Sources 196 (2011) 3949.
[14] J. Evans, C.A. Vincent, P.G. Bruce, Polymer 28 (1987) 2324.
[15] B.A. Boukamp, Solid State Ion. 20 (1986) 31.
[16] B.A. Boukamp, Solid State Ion. 18 & 19 (1986) 136.
[17] D. Chen, L. Cao, F. Huang, P. Imperia, Y.-B. Cheng, R.A. Caruso, J. Am. Chem. Soc. 132 (2010) 4438.
[18] D. Aurbach, J. Power Sources 89 (2000) 206.
[19] H. Ohno, M. Yoshizawa, W. Ogihara, Electrochim. Acta 48 (2003) 2079.
[20] J.Y. Song, Y.Y. Wang, C.C. Wan, J. Power Sources 77 (1999) 183.
[21] K. Thamaphat, P. Limuwan, B. Ngotawornchai, Nat. Sci. 42 (2008) 357.